ARTICLE

PV network plasticity mediated by neuregulin1-ErbB4 signalling controls fear extinction

Yi-Hua Chen[1,2,3], Neng-Yuan Hu[1,3], Ding-Yu Wu[1], Lin-Lin Bi[1], Zheng-Yi Luo[1], Lang Huang[1], Jian-Lin Wu[1], Meng-Ling Wang[1], Jing-Ting Li[1], Yun-Long Song[1], Sheng-Rong Zhang[1], Wei Jie[1], Xiao-Wen Li[1], Shi-Zhong Zhang[2], Jian-Ming Yang[1] and Tian-Ming Gao[1]✉

Neuroplasticity in the medial prefrontal cortex (mPFC) is essential for fear extinction, the process of which forms the basis of the general therapeutic process used to treat human fear disorders. However, the underlying molecules and local circuit elements controlling neuronal activity and concomitant induction of plasticity remain unclear. Here we show that sustained plasticity of the parvalbumin (PV) neuronal network in the infralimbic (IL) mPFC is required for fear extinction in adult male mice and identify the involvement of neuregulin 1-ErbB4 signalling in PV network plasticity-mediated fear extinction. Moreover, regulation of fear extinction by basal medial amygdala (BMA)-projecting IL neurons is dependent on PV network configuration. Together, these results uncover the local molecular circuit mechanisms underlying mPFC-mediated top-down control of fear extinction, suggesting alterative therapeutic approaches to treat fear disorders.

Molecular Psychiatry; https://doi.org/10.1038/s41380-021-01355-z

INTRODUCTION

Fear extinction, gradual reduction in the fear response by repeated presentation of nonreinforced fear-related cues, is the primary process used to overcome conditioned fear [1]. However, the mechanism by which fear memories are persistently weakened between exposure trials remains a major question. When extinction memories are formed, they are initially labile but become progressively consolidated into persistent traces. The consolidation of memories relies on both synaptic processes on a timescale of minutes to hours and circuit consolidation over weeks to years [2, 3]. Pioneering works have focused on the cellular mechanisms underlying fear extinction, including synaptic plasticity [4, 5]. In contrast, less attention has been given to the molecules and circuit elements controlling neuronal activity and the concomitant induction of plasticity during fear extinction.

Parvalbumin (PV)-positive GABAergic neurons are the predominant interneurons in the cortex [6]. They form synapses in the perisomatic and proximal dendritic regions of pyramidal neurons [7]. Local microcircuits involving inhibitory PV neurons regulate the activities of excitatory principal neurons, shape information processing and orchestrate the network activity flows that underlie animal behaviour [7, 8]. Moreover, it has been demonstrated that the differentiation state of PV neurons is involved in neuroplasticity during critical periods of cortical development [9–11] and in the adult hippocampus [12]. The medial prefrontal cortex (mPFC) is a key brain region for encoding and consolidating extinction memories [13, 14]. Lesions in the mPFC result in resistance to fear extinction [15]. Consistent with these results, electrical stimulation or optogenetic activation of the infralimbic (IL) subregion of the mPFC facilitates fear extinction [16, 17]. Although an increasing number of works have elucidated mPFC-connected brain regions in the regulation of fear extinction [18–21], the role of local network plasticity remains unclear. Here we explored the role of PV network plasticity in the regulation of fear extinction in the mPFC and the underlying molecular mechanisms.

RESULTS

Fear extinction learning induces PV network plasticity in the IL cortex

The fear extinction procedure employed in this study comprised four to six extinction trials with an interval time of days, which is traditionally used in the clinic to treat patients suffering from fear disorders, such as posttraumatic stress disorder and phobia [13, 22]. In this test, we conditioned mice by presenting a 30 s auditory tone (conditioned stimulus, CS), which co-terminated with a 1 s footshock for four trials. After fear retrieval, all mice were subjected to daily (24), every other day (48 h) or every 3 days (72 h) extinction trials for four to six consecutive trials. Each extinction trial consisted of a 3 min re-exposure to the CS without presenting footshock. During the extinction trainings, the rodents learn that the CS does not predict the aversive unconditioned stimulus (US) and form extinction memories for the previous extinction trainings. It is worth noting that the pre-CS freezing levels were consistent across all sessions (Supplementary Fig. 1a), indicating no change in motor behaviour after repeated CS

[1]State Key Laboratory of Organ Failure Research, Key Laboratory of Mental Health of the Ministry of Education, Guangdong-Hong Kong-Macao Greater Bay Area Centre for Brain Science and Brain-Inspired Intelligence, Guangdong Province Key Laboratory of Psychiatric Disorders, Department of Neurobiology, School of Basic Medical Sciences, Southern Medical University, Guangzhou 510515, China. [2]Department of Neurosurgery, Zhujiang Hospital, Southern Medical University, Guangzhou 510515, China. [3]These authors contributed equally: Yi-Hua Chen, Neng-Yuan Hu. ✉email: tgao@smu.edu.cn

Received: 13 April 2021 Revised: 2 October 2021 Accepted: 6 October 2021
Published online: 25 October 2021

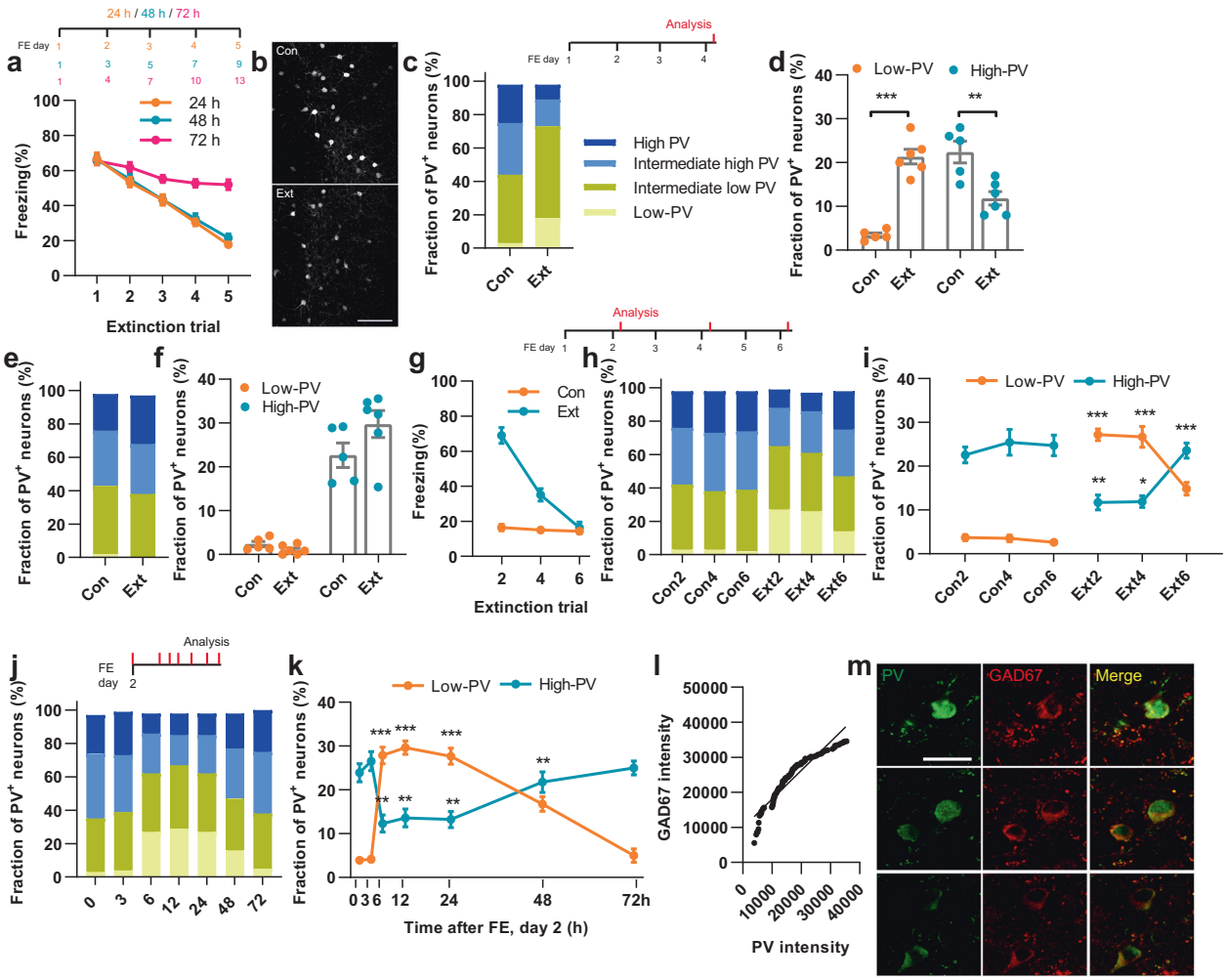

Fig. 1 Fear extinction induces low-PV plasticity in the IL cortex. a Extinction training conducted every day (24 h) or every other day (48 h) but not every 3 days (72 h) gradually extinguished fear memory. **b** Representative examples of PV immunocytochemistry under control conditions and after extinction. Scale bar = 100 µm. **c**, **d** Summary of PV network configuration in the IL cortex in the control group (con, $n = 5$ mice) and extinction group (ext, $n = 6$ mice). Low-PV, Welch's t-test (two-tailed), $t = 10.29$, df = 5.915, $p < 0.0001$; high-PV, unpaired t-test (two-tailed), $t = 3.74$, df = 9, $p = 0.005$. **e**, **f** Fear extinction did not affect PV network configuration in the PL cortex (con, $n = 5$ mice; ext, $n = 6$ mice). Low-PV, unpaired t-test (two-tailed), $t = 1.86$, df = 9, $p = 0.096$; high-PV, Kolmogorov–Smirnov test, $D = 0.67$, $p = 0.108$. **g** Fear extinction training gradually decreased freezing levels. **h**, **i** PV network configuration in the IL cortex on day 2 of extinction training (ext 2, con, $n = 6$ mice; ext, $n = 6$ mice), ext 4 (con, $n = 5$ mice; ext, $n = 6$ mice) and ext 6 (con, $n = 5$ mice; ext, $n = 6$ mice). Two-way ANOVA with Bonferroni's multiple comparisons test, group × time, F(2,28) = 5.34, $p = 0.0109$. **j**, **k** PV network configuration among mice at 0 h ($n = 5$ mice), 3 h ($n = 5$ mice), 6 h ($n = 6$ mice), 12 h ($n = 6$ mice), 24 h ($n = 6$ mice), 48 h ($n = 6$ mice) and 72 h ($n = 5$ mice) on day 2 after extinction training. Low-PV, Brown–Forsythe ANOVA test with Dunnett's T3 multiple comparisons, F(6,24.44) = 64.57, $p < 0.0001$; high-PV, one-way ANOVA test with Dunnett's multiple comparisons, F(6,32) = 9.31, $p < 0.0001$. **l**, **m** PV immunoreactivity in individual neurons was closely correlated with GAD67 immunoreactivity. From 107 neurons, Pearson's correlation, $r = 0.95$. Scale bar = 25 µm. Data are shown as the means ± SEM. $^{*}P < 0.05$, $^{**}P < 0.01$, $^{***}P < 0.001$. See Supplementary Table 1 for statistical details.

stimulus, and the CS after fear retrieval can trigger retrieval of extinction memories. Therefore, the freezing levels elicited by the CS are used as readouts of extinction memories acquired upon extinction learning [14, 23]. We found that the fear response gradually decayed in response to fear extinction training performed daily (24 h) or every other day (48 h) but not every 3 days (72 h) in naive mice (Fig. 1a), suggesting that extinction memory lasts for 2 days under the current protocol. In subsequent experiments, we adopted the daily training protocol, unless otherwise specified. To investigate the local circuit mechanism underlying this long-lasting memory, we compared the differentiation state of PV-positive neurons in the mPFC between fear extinction mice and nonextinction controls by analysing PV immunoreactivity (Supplementary Fig. 2), which has been reported to contribute to hippocampus-dependent remote memory [24]. Compared to the control group, mice with fear extinction exhibited a gradually decreasing fear response (Supplementary Fig. 1a), a robust increase in low-PV neurons and a reduction in high-PV neurons in the IL cortex (Fig. 1b–d and Supplementary Fig. 1b–e) but not in the prelimbic cortex (PL) cortex (Fig. 1e, f and Supplementary Fig. 1d). In contrast, mice that underwent fear retrieval displayed an increased percentage of high-PV neurons in the PL cortex (Supplementary Fig. 3a–c) but not in the IL cortex (Supplementary Fig. 3d–f). Next, we analysed the dynamic alterations of PV networks in the IL cortex as mice learned to extinguish fear memory. The learning phase of fear extinction was accompanied by a shift to a low-PV network configuration, whereas the establishment of robust extinction memory at the end of the learning protocol was accompanied by a shift back towards the baseline configuration (Fig. 1g–i and Supplementary Fig. 1g). Furthermore, we monitored a more detailed time course of the PV network configuration induced in

the IL cortex following fear extinction trail 2. We designated the time at which fear extinction trail 2 was completed as time +0 h. The distribution of PV-labelled neurons was not detectably altered up to +3 h and reached the highest low-PV values and the lowest high-PV values at +6 h. These values were maintained until +24 h and then decreased to half-maximal values for low-PV; the high-PV values reached the baseline levels at +48 h and the low-PV values reached baseline at +72 h (Fig. 1j, k and Supplementary Fig. 1h). Under all experimental conditions, PV immunoreactivity in individual interneurons was closely correlated with the immunoreactivity of GAD67 (Fig. 1l, m), which is a key GABA-synthesizing enzyme and a differentiation marker of PV neurons [25]. To validate our measurements, we used tdTomato as an internal staining control. We crossed PV-Cre mice with Ai14 tdTomato reporter mice to generate PV-Cre:Ai14 mice in which tdTomato was expressed in PV neurons. PV-Cre:Ai14 mice underwent fear extinction, which consistently induced an increase in the low-PV fraction in the IL cortex, as analysed by PV immunoreactivity, in parallel with constant tdTomato (anti-red fluorescent protein) staining (Supplementary Fig. 4a, b). In addition, as another control, we observed no changes in PV network plasticity in the piriform cortex, a brain region that has been shown not to be involved in fear-related behaviours [26] (Supplementary Fig. 4c–f). Taken together, these results indicate that fear extinction induces low-PV plasticity in the IL cortex.

Molecular and electrophysiological properties of low- and high-PV neurons

Next, we sought to identify any molecular distinctions between the low-PV and high-PV neuron populations in the mPFC. We began by analysing independent single-cell RNA sequencing data sets [27], which yielded differential gene ensembles according to Gene Ontology terms between low-PV and high-PV fractions, including ion transport, voltage-gated ion channel, vesicle-mediated transport, GABAergic synaptic transmission, calcium ion transmembrane transport and nervous system development

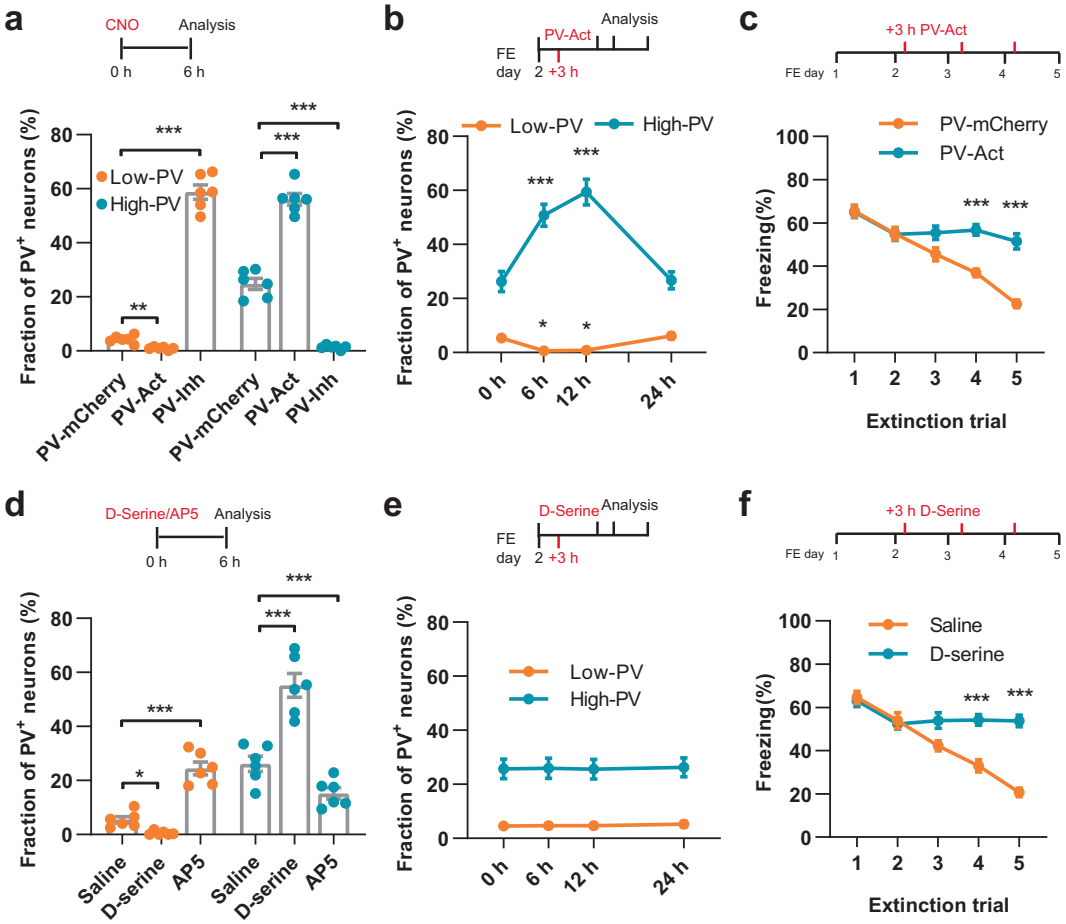

Fig. 2 Sustained low-PV plasticity in the IL cortex is required for fear extinction. a Chemogenetic manipulation (PV-Act, hM3Dq-mCherry; PV-Inh, hM4Di-mCherry) of PV neurons bidirectionally modulated PV network configuration ($n = 6$ mice for each group). Low-PV, Brown–Forsythe ANOVA test with Tamhane's T2 multiple comparisons test, $F(2,5.56) = 434.8$, $p < 0.0001$; high-PV, one-way ANOVA with Dunnett's multiple comparisons, $F(2,15) = 258.2$, $p < 0.0001$. **b**, **c** Interference with low-PV configuration (**b**) following fear extinction by delivery of a chemogenetic ligand (CNO) at +3 h suppressed fear extinction (**c**). **b** $n = 6$ mice for each group, low-PV, Brown–Forsythe ANOVA test with Dunnett's T3 multiple comparisons, $F(3,11.50) = 12.23$, $p = 0.0007$; high-PV, one-way ANOVA with Dunnett's multiple comparisons, $F(3,20) = 18.10$, $p < 0.0001$. **c** $n = 9$ mice for each group, two-way repeated-measures ANOVA with Bonferroni's multiple comparisons test, group × time, $F(4,64) = 10.87$, $p < 0.0001$. **d** Pharmacological manipulation of the NMDA receptor (co-agonist, D-serine; antagonist, AP5) bidirectionally modulated PV network configuration ($n = 6$ mice for each group). Low-PV, Brown–Forsythe ANOVA test with Dunnett's T3 multiple comparisons, $F(2,7.48) = 66.32$, $p < 0.0001$; high-PV, one-way ANOVA with Dunnett's multiple comparisons, $F(2,15) = 40.27$, $p < 0.0001$. **e**, **f** Interference with low-PV configuration (**e**) following fear extinction by delivery of D-serine at +3 h suppressed fear extinction (**f**). **e** $n = 6$ mice for each group, low-PV, one-way ANOVA, $F(3,20) = 0.08$, $p = 0.9706$; high-PV, Kruskal–Wallis test, $H(3,24) = 0.18$, $p = 0.9808$. **f** $n = 8$ mice for each group, two-way repeated-measures ANOVA with Bonferroni's multiple comparisons test, group × time, $F(4,56) = 17.75$, $p < 0.0001$. Data are shown as the means ± SEM. *$P < 0.05$, **$P < 0.01$, ***$P < 0.001$. See Supplementary Table 1 for statistical details.

(Supplementary Fig. 5). Given that fear extinction induced higher fractions of low-PV neurons, we examined the expression changes of some of the above differential genes from PV neurons sorted at +6 h post extinction using digital droplet PCR (ddPCR) (Supplementary Fig. 6a, b). We found that the genes enriched in low-PV fractions were more highly expressed, whereas the genes enriched in high-PV fractions were reduced after fear extinction (Supplementary Fig. 6c), suggesting that extinction induces a low-PV state comprising changes in PV and other functional molecules.

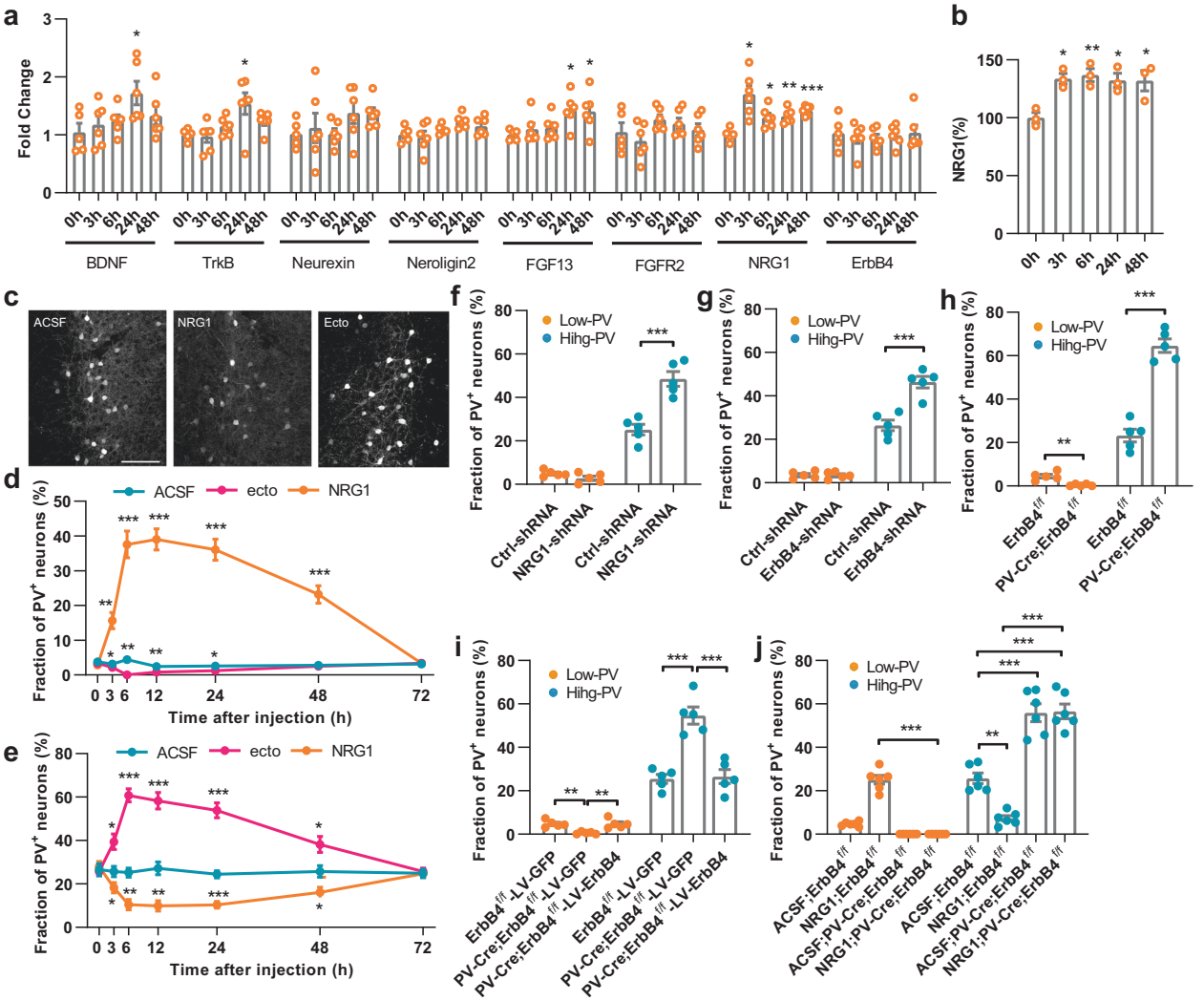

Fig. 3 PV network plasticity is sustained through NRG1-ErbB4 signalling. a Measurements of the mRNA levels of BDNF, TrkB, Neurexin, Neuroligin2, FGF13, fibroblast growth factor receptor 2 (FGFR2), NRG1 and ErbB4 in the mPFC 2 days following fear extinction ($n = 5$ mice for 0 h; $n = 6$ mice each for 3, 6, 24 and 48 h). BDNF, one-way ANOVA with Dunnett's multiple comparisons test, $F(4, 24) = 2.63$, $p = 0.0593$; TrkB, Kruskal–Wallis test with Dunn's multiple comparisons test, $H(4, 29) = 10.13$, $p = 0.0382$; Neurexin, one-way ANOVA test, $F(4, 24) = 2.63$, $p = 0.0593$; Neuroligin2, one-way ANOVA test, $F(4, 24) = 2.77$, $p = 0.0502$; FGF13, one-way ANOVA with Dunnett's multiple comparisons test, $F(4, 24) = 3.29$, $p = 0.0275$; FGFR2, one-way ANOVA test, $F(4, 24) = 1.66$, $p = 0.1926$; NRG1, Brown–Forsythe ANOVA test with Dunnett's T3 multiple comparisons test, $F(4, 10.27) = 66.32$, $p = 0.0023$; and ErbB4, one-way ANOVA test, $F(4, 24) = 0.17$, $p = 0.9491$. **b** Western blot analysis showing that NRG1 levels increased following fear extinction trail 2 ($n = 3$ mice for each group). One-way ANOVA with Dunnett's multiple comparisons test, $F(4, 10) = 6.13$, $p = 0.0093$. **c**–**e** The percentage of low-PV (**d**) and high-PV neurons (**e**) at 0 h ($n = 6$, 6 and 5 mice for ACSF, Ecto and NRG1, respectively), 3 h ($n = 6$ mice for each group), 6 h ($n = 5$, 6 and 6 mice for ACSF, Ecto and NRG1, respectively), 12 h ($n = 6$ mice for each group), 24 h ($n = 6$ mice for each group), 48 h ($n = 6$ mice for each group) and 72 h ($n = 5$, 6 and 6 mice for ACSF, Ecto and NRG1, respectively) after IL administration of artificial cerebrospinal fluid (ACSF), NRG1 and Ecto-ErbB4 (Ecto). Low-PV, two-way ANOVA with Dunnett's multiple comparisons test, group × time, $F(12,101) = 36.94$, $p < 0.0001$; high-PV, two-way ANOVA with Dunnett's multiple comparisons test, group × time, $F(12,101) = 17.78$, $p < 0.0001$. Scale bar = 100 μm. **f** Knockdown of NRG1 in the IL cortex induced an increase in the high-PV percentage ($n = 5$ mice for each group). Low-PV, unpaired *t*-test (two-tailed), $t = 1.79$, df = 8, $p = 0.1113$; high-PV, unpaired *t*-test (two-tailed), $t = 5.62$, df = 8, $p = 0.0005$. **g** Knockdown of ErbB4 from PV neurons in the IL cortex induced an increase in the high-PV percentage ($n = 5$ mice for each group). Low-PV, unpaired *t*-test (two-tailed), $t = 0.13$, df = 8, $p = 0.8985$; high-PV, unpaired *t*-test (two-tailed), $t = 5.54$, df = 8, $p = 0.0005$. **h** PV-Cre;ErbB4f/f mice showed a lower low-PV fraction and a higher high-PV fraction in the IL cortex ($n = 5$ mice for each group). Low-PV, Welch's *t*-test (two-tailed), $t = 4.70$, df = 4.68, $p = 0.006$; high-PV, unpaired *t*-test (two-tailed), $t = 9.70$, df = 8, $p < 0.0001$. **i** Overexpression of ErbB4 in the IL cortex restored the PV configuration of PV-Cre;ErbB4f/f mice ($n = 5$ mice for each group). Low-PV, one-way ANOVA with Tukey's multiple comparisons test, $F(2,12) = 12.34$, $p = 0.0012$; high-PV, one-way ANOVA with Tukey's multiple comparisons test, $F(2,12) = 27.13$, $p < 0.0001$. **j** IL administration of NRG1 had no effects on PV configuration in PV-Cre;ErbB4f/f mice ($n = 5$ mice for each group). Low-PV, Kruskal–Wallis test with Dunn's multiple comparisons test, $H(3,24) = 22.20$, $p < 0.0001$; high-PV, one-way ANOVA with Tukey's multiple comparisons test, $F(3,20) = 65.40$, $p < 0.0001$. Data are shown as the means ± SEM. $^*P < 0.05$, $^{**}P < 0.01$, $^{***}P < 0.001$. See Supplementary Table 1 for statistical details.

Furthermore, we explored the electrophysiological properties between low- and high-PV neurons. PV neurons were visualized using tdTomato in PV-Cre:Ai14 mice. We performed whole-cell recording combined with single-cell ddPCR and found that PV transcripts in individual neurons were closely correlated with GAD67 transcripts but had no correlation with the intrinsic electrophysiological properties of PV neurons (Supplementary Fig. 6d–k). Then, we directly examined the synaptic inputs from PV neurons to pyramidal neurons in the IL cortex by performing patch-clamp recording combined with optogenetic activation of ChR2-expressing PV fibres after fear extinction (Supplementary Fig. 6l) and found that the evoked responses were reduced at higher stimulus intensities (Supplementary Fig. 6m), accompanied by a higher paired-pulse ratio at +12 h post extinction than at +3 h (Supplementary Fig. 6n), a time point at which there were no alterations in PV immunoreactivity (Fig. 1j, k), indicating that fear extinction weakens the functional outputs of PV neurons, in accordance with a low-PV network configuration.

Together, these results suggest that PV network plasticity in the IL cortex may underlie fear extinction.

Low-PV configuration is required for extinction learning

To determine whether PV network configuration shifts in the IL cortex are sufficient to modulate extinction learning, we locally interfered with the low-PV shift following fear extinction. In the first set of experiments, we implemented a chemogenetic approach using designer receptors exclusively activated by designer drugs [28–30] to manipulate the PV network configuration in vivo. hM4Di or hM3Dq, engineered G protein-coupled receptors that suppressed or enhanced neuronal activity, respectively, in the presence of its agonist clozapine-N-oxide (CNO), was expressed in PV neurons using bilateral injection of AAV-DIO-hM4Di-mCherry (PV-Inh) or AAV-DIO-hM3Dq-mCherry (PV-Act) into the IL of PV-Cre mice (Supplementary Fig. 7a, b). Infusions of CNO (5 μM) into the IL slices from these mice resulted in a marked decrease (PV-Inh) or increase (PV-Act) in firing activity (Supplementary Fig. 7c), an indication of functional expression of hM4Di or hM3Dq, respectively. Chemogenetic inhibition of PV neurons was sufficient to induce a low-PV network configuration, whereas PV neuronal activation led to a high-PV network configuration (Fig. 2a and Supplementary Fig. 1i, j). Chemogenetic imposition of a high-PV shift at +3 h following fear extinction suppressed the low-PV shift (Fig. 2b and Supplementary Fig. 1k, l) and previous learning (Fig. 2c). To exclude any action of CNO at a dosage used in the above experiments (5 mg/kg) and its metabolites on PV network plasticity and fear extinction, we also examined the effects of CNO on PV-Cre mice injected with control virus and found no differences between saline- and CNO-treated mice (Supplementary Fig. 7d–g). In the second approach, we delivered the *N*-methyl-D-aspartate receptor antagonist AP5 and co-agonist D-serine to manipulate the PV network configuration [31]. AP5 was sufficient to induce a low-PV network configuration, whereas D-serine led to a high-PV network configuration (Fig. 2d and Supplementary Fig. 1m, n). Delivery of D-serine at +3 h following fear extinction suppressed the low-PV shift (Fig. 2e and Supplementary Fig. 1o, p) and previous learning (Fig. 2f). These observations demonstrate that the PV network configuration regulates extinction learning.

PV network plasticity is sustained through NRG1-ErbB4 signalling

To characterize the molecular mechanisms that underlie PV network plasticity in fear extinction, we analysed the mRNA levels of factors known to regulate the development and function of GABAergic neurons following fear extinction (Fig. 3a and Supplementary Fig. 8a). mPFC tissues were collected at different time points (from +0 h to +48 h) after fear extinction and mRNA levels were analysed using quantitative PCR (qPCR). The mRNA levels of brain-derived neurotrophic factor, TrkB and fibroblast growth factor 13 were increased at +24 h (Fig. 3a.). Notably, neuregulin 1 (NRG1) mRNA levels were significantly increased at +1 h and were sustained until +48 h (Fig. 3a and Supplementary Fig. 8b), and a similar change in NRG1 protein expression with a delay of 2 h was observed by western blotting (Fig. 3b and Supplementary Fig. 8c). As fear extinction-induced PV network plasticity was specifically restricted to the IL cortex but not the PL cortex, we further separated the PL and IL cortices, and detected NRG1 levels in these respective tissues. qPCR showed that NRG1 mRNA levels were exclusively increased in the IL cortex after fear extinction (Supplementary Fig. 8d, e). Taken together with our observations that extinction-induced PV network plasticity appear at +6 h and are maintained until +48 h (Fig. 1j, k), the expression patterns of the NRG1 protein suggest that it may play a role in fear extinction.

NRG1, which belongs to a family of growth factors that contain the epidermal growth factor-like domain, plays a critical role in neural development, synaptic plasticity and neuronal survival [32]. NRG1 exerts its function by activating ErbB tyrosine kinases (ErbB2–4), among which ErbB4 is the only tyrosine kinase that can both bind to NRG1 and become a functionally active homodimer [32]. To determine whether NRG1 modulates PV network plasticity, we monitored the time course of the PV configuration changes induced using three strategies to manipulate NRG1 activity in the IL cortex. First, we managed to block endogenous NRG1 signalling by applying ecto-ErbB4 (Ecto) (Supplementary Fig. 8f), which is a soluble polypeptide that contains the full extracellular domain of ErbB4 and can bind to and neutralize NRG1 [33]. We designated the time at which Ecto injection was completed as time +0 h. After Ecto injection, the high-PV configuration was detectably altered at +3 h, reached a peak at +6 h, remained at the peak level until +24 h, decreased to half-maximal values at +48 h and reached baseline at +72 h (Fig. 3c–e and Supplementary Fig. 1q, r). Next, we examined whether the application of exogenous NRG1 has any effect on the PV network configuration. Using the same protocol, we found that NRG1 induced a low-PV configuration in a similar time pattern as the high-PV configuration of Ecto (Fig. 3c–e and Supplementary Fig. 1q, r). In contrast to IL, NRG1 had no effect on the PV network configuration, whereas ecto induced an increase in the high-PV fraction in the PL cortex (Supplementary Fig. 8g–j). To further determine whether NRG1 was sufficient to regulate PV network plasticity, we employed AAV2/2 viral vectors to express a short hairpin RNA (shRNA) to knock down expression levels of NRG1. Stereotactic delivery of the NRG1-shRNA-mChery vectors resulted in IL-specific expression (Supplementary Fig. 8k). According to the western blot analysis, NRG1-shRNA depleted NRG1 expression 3 weeks after injection (Supplementary Fig. 8l). In agreement with the results of ecto treatment, knockdown of NRG1 induced an increase in the high-PV fraction (Fig. 3f and Supplementary Fig. 1s, t). These results suggest a critical role of NRG1 signalling in regulating the PV state.

To determine whether ErbB kinases in the IL cortex are involved in the modulation of PV network plasticity, we employed the ErbB kinase inhibitors AG1478 (AG) and PD158780 (PD), and found that both PD and AG induced an increase in the high-PV fraction (Supplementary Fig. 9a–c).

ErbB4 has been detected in PV+ neurons in the prefrontal cortex and hippocampus [34–36]. To further validate this finding, we generated ErbB4-reporter mice by crossing ErbB4–2A-CreERT2 mice, which express Cre recombinase under the ErB4 promoter in a tamoxifen-inducible manner, with Ai14 mice in which tdTomato transcription from the Rosa 26 locus was prevented by a loxP-flanked STOP cassette. We observed that a total of ~68% of PV+ neurons were positive for ErbB4 in the IL cortex (Supplementary Fig. 9d). To determine whether ErbB4 in PV neurons is necessary for PV network plasticity, we specifically knocked down ErbB4 expression using AAV2/2 viral vectors to express a floxed shRNA (AAV-DIO- ErbB4-

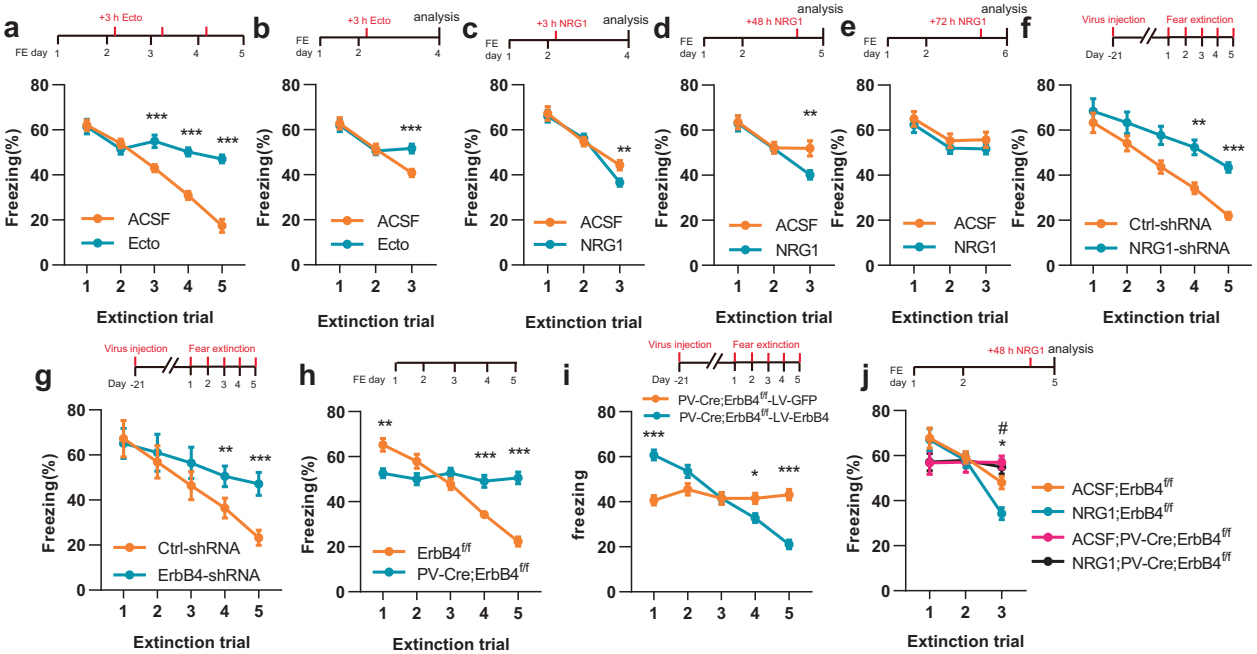

Fig. 4 NRG1-ErBb4 signalling regulates fear extinction. a, **b** IL infusion of Ecto-ErbB4 (Ecto) impaired fear extinction ($n = 12$ mice for each group). **a** Two-way repeated-measures ANOVA with Bonferroni's multiple comparisons test, group × time, $F(4,88) = 15.94$, $p < 0.0001$. **b** Unpaired *t*-test (two-tailed), $t = 4.20$, $df = 22$, $p = 0.0003$. **c**–**e** IL infusion of NRG1 at +3 h (**c**) or +48 h (**d**) but not +72 h (**e**) facilitated fear extinction. **c** $n = 12$ mice for each group, unpaired *t*-test (two-tailed), $t = 2.91$, $df = 22$, $p = 0.0082$; **d** $n = 8$ mice for each group, unpaired *t*-test (two-tailed), $t = 3.00$, $df = 14$, $p = 0.0095$; **e** $n = 8$ mice for each group, Mann–Whitney test, $U = 25$, $p = 0.5053$. **f** Knockdown of NRG1 in the IL impaired fear extinction ($n = 8$ mice for each group). Two-way repeated-measures ANOVA with Bonferroni's multiple comparisons test, group × time, $F(1,14) = 39.74$, $p = 0.0095$. **g** Knockdown of ErbB4 in PV neurons in the IL impaired fear extinction ($n = 8$ mice for each group). Two-way repeated-measures ANOVA with Bonferroni's multiple comparisons test, group × time, $F(4,56) = 6.74$, $p = 0.0002$. **h** PV-Cre;ErbB4f/f mice exhibited impaired fear extinction ($n = 10$ mice for each group). Two-way repeated-measures ANOVA with Bonferroni's multiple comparisons test, group × time, $F(4,36) = 24.92$, $p < 0.0001$. **i** IL overexpression of ErbB4 rescued the impaired fear extinction in PV-Cre;ErbB4f/f mice ($n = 10$ mice for each group). Two-way repeated-measures ANOVA with Bonferroni's multiple comparisons test, group × time, $F(4,72) = 23.70$, $p < 0.0001$. **j** IL administration of NRG1 had no effect on fear extinction in PV-Cre;ErbB4f/f mice. Data are shown as the means ± SEM. $^*P < 0.05$, $^{**}P < 0.01$, $^{***}P < 0.001$. See Supplementary Table 1 for statistical details.

shRNA-mCherry) in PV-Cre mice. Three weeks after the injection, ErbB4-shRNA was specifically expressed in PV neurons and western blot analysis showed that expression levels of ErbB4 were significantly lower in the mPFC (Supplementary Fig. 9e–g). We performed PV immunostaining in IL slices from AAV-DIO- ErbB4-shRNA-mCherry and AAV-DIO nonsense-shRNA-mCherry-treated PV-Cre mice and found that knockdown of ErbB4 in PV neurons induced a high-PV configuration (Fig. 3g and Supplementary Fig. 1u, v). We also examined PV-Cre:ErbB4$^{f/f}$ mice [34, 37], in which ErbB4 levels in the mPFC were reduced (Supplementary Fig. 9h). Consistent with the results of the ErbB4-shRNA experiment, ablation of ErbB4 in PV+ neurons induced a high-PV configuration in the IL cortex (Fig. 3h and Supplementary Fig. 1w, x).

Given our observations that both shRNA treatment and conditional knockout mice displayed a high-PV configuration, we hypothesized that ErB4 expression in the IL cortex was required for PV network plasticity. To test this hypothesis, we generated a lentivirus (LV) ErbB4 expression vector (LV-ErbB4) [33]. LV-ErbB4 was bilaterally infused into the IL cortex of PV-Cre:ErbB4$^{f/f}$ mice (Supplementary Fig. 9i) and tissues were collected 3 weeks later. Western blottings confirmed successful overexpression of the ErbB4 protein in the IL cortex (Supplementary Fig. 9j). Then, we examined the consequences of ErbB4 overexpression on PV network plasticity. PV-Cre:ErbB4$^{f/f}$ mice exhibited a high-PV configuration. LV-mediated ErbB4 overexpression in the IL cortex of PV-Cre:ErbB4$^{f/f}$ mice significantly restored the increase in the high-PV configuration (Fig. 3i and Supplementary Fig. 1y, z).

To determine whether NRG1 regulates the PV network state via ErbB4, we administered NRG1 into the IL cortex of PV-Cre:ErbB4$^{f/f}$ mice and their littermate controls. NRG1 induced a low-PV configuration in control mice but this effect was totally blocked by ErbB4 ablation from PV neurons (Fig. 3j and Supplementary Fig. 1ab, ac), suggesting that NRG1 regulates the PV network state via ErbB4.

Given our observations that exogenous NRG1 induced low-PV network plasticity in the IL cortex but had no effects on PV network plasticity in the PL cortex, we speculated that NRG1-ErbB4 activity is saturated in the PL cortex. To test this hypothesis, we examined the levels of ErbB4 and its phosphorylation, indicative of ErbB4 activation, in the respective tissues and found that the levels of both ErbB4 and phospho-ErbB4 were higher in the PL cortex than in the IL cortex (Supplementary Fig. 10). Importantly, stimulation with exogenous NRG1 increased phospho-ErbB4 in the IL cortex but not the PL cortex, supporting saturated NRG1-ErbB4 activity in the PL. These results, together with our prior data (Supplementary Fig. 8d, e), suggested that fear extinction increased NRG1 expression specifically in the IL cortex, which further activated ErbB4 and consequently induced low-PV plasticity. In contrast, no change occurring in PV plasticity in the PL cortex following extinction may be due to both saturated NRG1-ErbB4 activity and unchanged NRG1 levels.

NRG1-ErbB4 signalling in PV neurons contributes to fear extinction

To determine whether NRG1 signalling modulates fear extinction, we used the same strategies as described above (Fig. 4) to manipulate NRG1 activity in the IL cortex. Ecto or NRG1 was infused +3 h post extinction to avoid acute effects. First,

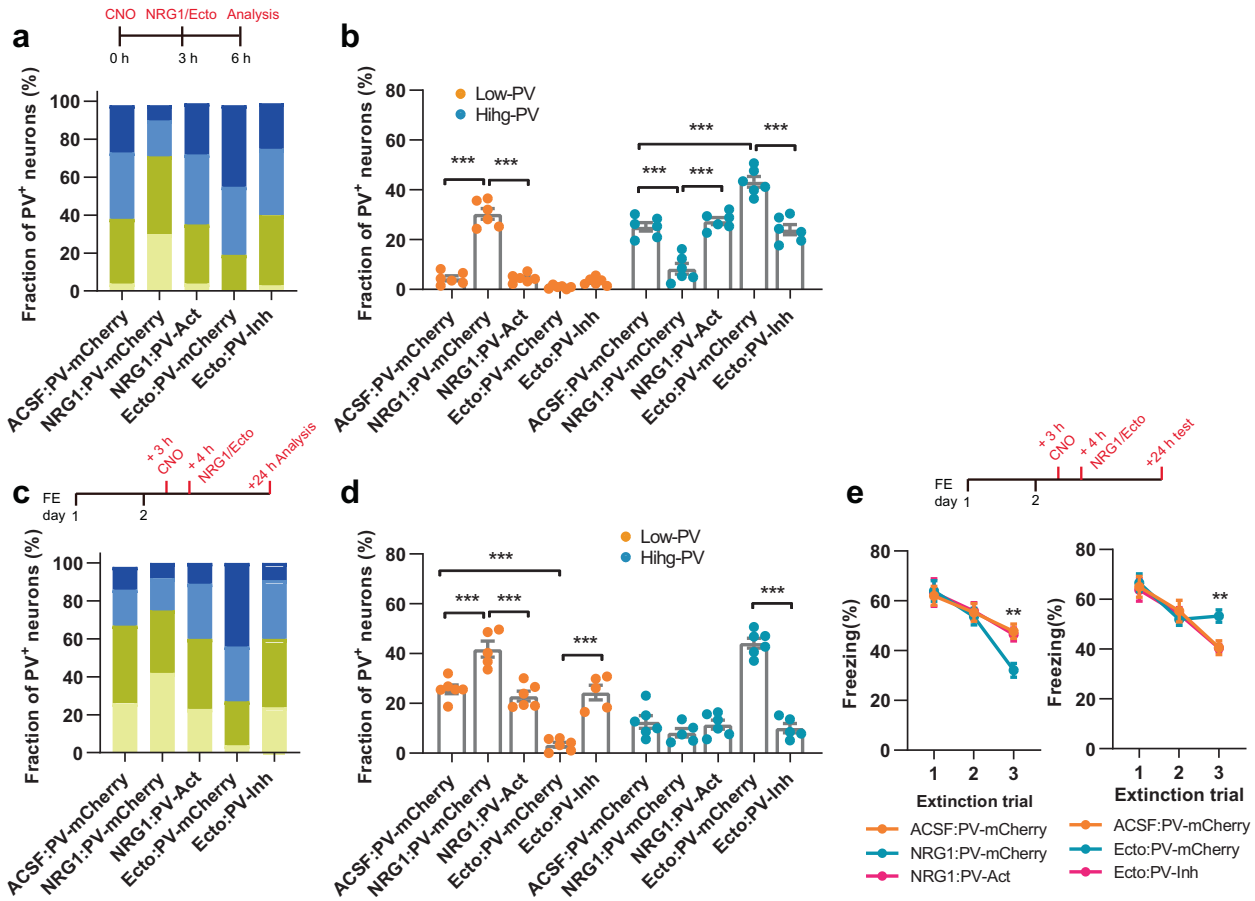

Fig. 5 NRG1 signalling regulates fear extinction by modulating PV network plasticity. a, **b** Interference with the PV configuration using chemogenetics blocked the effect of NRG1 or Ecto-ErbB4 on PV network plasticity ($n = 6$ mice for each group). Low-PV, Brown–Forsythe ANOVA test with Dunnett's T2 multiple comparisons test, $F(4,9.75) = 113.3$, $p < 0.0001$; high-PV, one-way ANOVA test with Tukey's multiple comparisons test, $F(4,25) = 42.87$, $p < 0.0001$. **c**–**e** Interference with PV configuration using chemogenetics following fear extinction blocked the effect of NRG1 or Ecto-ErbB4 on PV network plasticity (**c**, **d**) and fear extinction (**e**). **c**, **d** $n = 6$, 5, 6, 6 and 5 mice for the ACSF:PV-mCherry, NRG1:PV-mCherry, NRG1:PV-Act, Ecto:PV-mCherry and Ecto:PV-Inh groups, respectively. Low-PV, one-way ANOVA test with Tukey's multiple comparisons test, $F(4,23) = 39.08$, $p < 0.0001$; high-PV, one-way ANOVA test with Tukey's multiple comparisons test, $F(4,23) = 57.15$, $p < 0.0001$. **e** Left, $n = 8$, 9, 8 mice for the ACSF:PV-mCherry, NRG1:PV-mCherry and NRG1:PV-Act groups, respectively; one-way ANOVA test with Tukey's multiple comparisons test, $F(2,22) = 10.16$, $p = 0.0008$; right, $n = 8$ mice for each group; one-way ANOVA test with Tukey's multiple comparisons test, $F(2,21) = 10.21$, $p = 0.0008$. Data are shown as the means ± SEM. $^{*}P < 0.05$, $^{**}P < 0.01$, $^{***}P < 0.001$. See Supplementary Table 1 for statistical details.

neutralizing NRG1 using local delivery of Ecto to IL suppressed fear extinction (Fig. 4a) and this inhibitory effect lasted up to 48 h (Fig. 4b). Second, application of exogenous NRG1 to IL at +3 or +48 h facilitated fear extinction (Fig. 4c, d), but this facilitation disappeared when NRG1 was supplied at +72 h (Fig. 4e). The time window of extinction modulation was in accordance with the effects of NRG1 signalling on PV network plasticity. We next examined the effect of NRG1-shRNA on fear extinction and found that, in line with the Ecto treatment results, knockdown of NRG1 in the IL cortex slowed the extinction process (Fig. 4f). These observations suggest that NRG1 signalling has a role in modulating extinction in the IL cortex.

To test whether ErbB4 in PV neurons is necessary for fear extinction, we first examined the effect of ErbB4-shRNA on fear extinction and found that knockdown of ErbB4 in PV neurons in the IL cortex impaired fear extinction (Fig. 4g). We next implemented PV-Cre:ErbB4$^{f/f}$ mice. Consistent with the previous results, PV-Cre:ErbB4$^{f/f}$ mice exhibited difficulty extinguishing fear memory (Fig. 4h). However, this deficit was reversed by LV-mediated ErbB4 overexpression in the IL cortex in PV-Cre:ErbB4f/f mice (Fig. 4i), suggesting that ErbB4 in PV neurons is required for fear extinction. To determine whether NRG1 facilitates fear extinction via ErbB4 activation, we injected NRG1 into the IL cortices of PV-Cre:ErbB4$^{f/f}$ mice and found that the facilitating effect of NRG1 disappeared (Fig. 4j). These results demonstrate that ErbB4 in PV neurons is essential for the NRG1-mediated modulation of fear extinction.

NRG1 signalling regulates fear extinction by modulating PV network plasticity

To determine whether NRG1 signalling-mediated fear extinction depends on shifts in PV network configuration, we conducted experiments in which we combined the imposition of PV plasticity using chemogenetics with manipulation of NRG1 signalling. Given that pharmacogenetically induced PV plasticity became detectable at +6 h, whereas NRG1 signalling appears at +3 h, we locally delivered NRG1 at +3 h after pharmacogenetic stimulation. We found that enhancing PV neuronal activity by CNO prevented NRG1-induced shifts in the PV network configuration in naive mice (Fig. 5a, b and Supplementary Fig. 11a). In mice in which an additional low-PV shift was induced by NRG1 injection in IL at +4 h after extinction, delivery of CNO at +3 h blocked these effects (Fig. 5c, d and Supplementary Fig. 11b) and further blocked NRG1's facilitation of fear extinction (Fig. 5e). Similarly,

chemogenetically inhibiting PV neurons prevented Ecto-ErbB4-triggered shifts in the PV network configuration in both naive mice (Fig. 5a, b and Supplementary Fig. 11a) and mice trained with fear extinction (Fig. 5c, d and Supplementary Fig. 11b), and was also sufficient to suppress the impairment of fear extinction induced by Ecto-ErbB4 (Fig. 5e). Taken together, these results suggest that NRG1 signalling-mediated PV network plasticity in the IL cortex is critical for fear extinction.

To determine whether NRG1 signalling is generally important in learning-related PV plasticity, we used another learning task known as inhibitory avoidance (IA) learning. We first analysed changes in both PV networks and NRG1 expression in hippocampal CA1 after the IA task. IA training produced a major shift to a low-PV network configuration in CA1 (Supplementary Fig. 12a–d) accompanied by increased NRG1 mRNA levels (Supplementary Fig. 12e, f). Moreover, application of NRG1 at +3 h promoted the training-induced low-PV state (Supplementary Fig. 12g–i) and facilitated memory retention (Supplementary Fig. 12j, k), whereas the ErbB4 antagonist AG induced the opposite effects. These results suggest that NRG1 signalling-mediated PV plasticity is required for at least two different kinds of learning.

PV network plasticity in the IL cortex is involved in the top-down control of fear extinction

Previous work has reported that the basomedial amygdala (BMA) represents a major target of the ventral medial prefrontal cortex (vmPFC), including the IL cortex, and activation of BMA-projecting neurons mediates fear extinction [18]. Therefore, we explored whether PV neuronal plasticity in the IL cortex is required for BMA-projecting IL neurons to modulate fear extinction. To determine whether IL neurons directly innervated the BMA, we injected the retrograde tracer RetroBeads into the BMA of C57 mice (Supplementary Fig. 13a) and observed that a considerable number of neurons were labelled with beads in the IL cortex 2 weeks later (Fig. 6a). We then investigated the time course of c-Fos expression in BMA-projecting IL neurons following fear extinction. In addition to an early peak approximately +1.5 h after fear extinction on day 2, the fractions of c-Fos$^+$beads$^+$ cells peaked again at +10 h and were maintained for 5 h, suggesting extinction-induced activation of BMA-projecting IL neurons. To test the involvement of this circuit in fear extinction, we used chemogenetics to inhibit BMA-projecting IL neurons. We targeted these neurons by injecting the retrogradely propagating canine adenovirus encoding Cre recombinase into the BMA and directing AAV-DIO-hM4DGi-mCherry expression in the IL (Supplementary Fig. 13e), and found that chemogenetic inhibition at +8 h impaired fear extinction (Fig. 6c). To investigate whether the low-PV transition is sufficient to trigger BMA-projecting neuron activation, we injected cholera toxin subunit B (CTB) in BMA and AAV-DIO-hM4DGi-mCherry or AAV-DIO-mCherry as a control in the IL cortex of PV-Cre mice (Supplementary Fig. 13f, g). Chemogenetic imposition of a low-PV shift in the IL cortex induced an increase in Fos$^+$CTB$^+$ cells (Fig. 6d). Consistent with the notion that sustained PV plasticity is necessary for fear extinction, chemogenetic activation of PV neurons at +3 h abolished the c-Fos peak at +10 h (Fig. 6e) and impaired fear extinction (Fig. 6f). To clarify the specificity of the IL-BMA network, we chose another amygdala targeting population, CeA-projecting IL neurons, a recently identified pathway involved in fear extinction [38], and evaluated whether it might be influenced by low-PV plasticity. We found that CeA-projecting neurons were activated only at the first c-fos peak but, in contrast to BMA-projecting IL neurons, not at the second c-fos peak following fear extinction (Supplementary Fig. 13b–d), which is required for extinction and controlled by PV network plasticity (Fig. 6e, f). Taken together, these results suggest that PV neuronal plasticity in the IL cortex is involved in the top-down control of fear extinction with pathway specificity among the amygdala targets.

DISCUSSION

Collectively, our data reveal that fear extinction induces sustained plasticity of the PV neuron network accompanied by elevated expression of NRG1 in the IL but not the PL subregion of the mPFC in adult mice. Gain or loss of NRG1 or its receptor ErbB4 bidirectionally regulated PV network plasticity and fear extinction. Moreover, the regulation of fear extinction by NRG1-ErbB4 signalling in PV neurons was dependent on PV network configuration. Notably, excitation of BMA-projecting IL neurons was dependent on PV network configuration and contributed to fear extinction. Together, these results uncover the molecular and local circuit mechanisms for the mPFC-mediated top-down control of fear extinction.

Our findings are consistent with early reports that extinction-related plasticity in the IL mPFC is important for fear extinction [13, 14]. To elucidate the local circuit mechanism by which IL plasticity regulates extinction, we took advantage of the employed experimental procedure using an interval time of 24 h and observed a reconstruction of the PV network configuration after two trials that was dependent on NRG1-ErbB4 signalling. Interference with PV configuration shifts following extinction blocked both extinction-induced PV network plasticity and previous extinction learning, indicating that extinction-induced PV network plasticity is required for extinction. Alterations in PV configuration were detected +6 h after extinction and were maintained through +48 h, which is the time window of memory consolidation processes, consistent with the notion that memory consolidation might involve local network activity [24, 39].

Notably, the differentially expressed genes in the high-PV fraction were involved in functions including ion transport, voltage-gated ion channels, vesicle-mediated transport and GABAergic synaptic transmission, whereas the genes in the low-PV fraction were involved in calcium ion transmembrane transport and nervous system development, indicating that high-PV neurons are mature cells, whereas low-PV neurons are immature cells [7, 40]. We further analysed gene expression in PV neurons from control and extinction learning mice. In the extinction sample, those neurons contained higher fractions of low-PV neurons and exhibited molecular features consistent with low-PV neurons. Notably, as neurons from extinction samples still constituted a mixed population of low- and high-PV neurons, those altered genes upon extinction learning may also be related to processes other than low-PV plasticity. Further efforts should be made to develop new techniques to isolate and interfere with low- and high-PV fractions. Importantly, the extinction-induced low-PV configuration recapitulated the electrophysiological properties, indicating the immature state of low-PV neurons. Specifically, among the genes downregulated after fear extinction, GAD67 is a key GABA-synthesizing enzyme [25]. VAMP1, a member of the vesicle-associated membrane protein (VAMP)/synaptobrevin family, plays a role in the packaging, transport or release of neurotransmitters [41]. Vps33a is a member of the Sec1 and Class C multiprotein complex whose correct assembly is required for the normal function of intracellular protein trafficking from the Golgi to the vacuole [42, 43]. Loss of Sec1 function results in a reduction in the evoked synaptic response and impairs synaptic vesicle trafficking at multiple steps, ultimately affecting neurotransmitter release [44]. Therefore, it is possible that NRG1/ErbB4 signalling may downregulate these functional molecules, resulting in weakened GABA release of PV neurons following fear extinction. Given this, our study and others [45–47] support the idea that PV neuron properties are malleable in the adult cortex, at least to a certain extent.

A key finding of the present study is that NRG1-ErbB4 signalling-mediated fear extinction depends on shifts in the PV network configuration. Notably, the low-PV configuration only became detectable 6 h after extinction, whereas NRG1 protein levels increased 3 h earlier. These results thus suggest that the

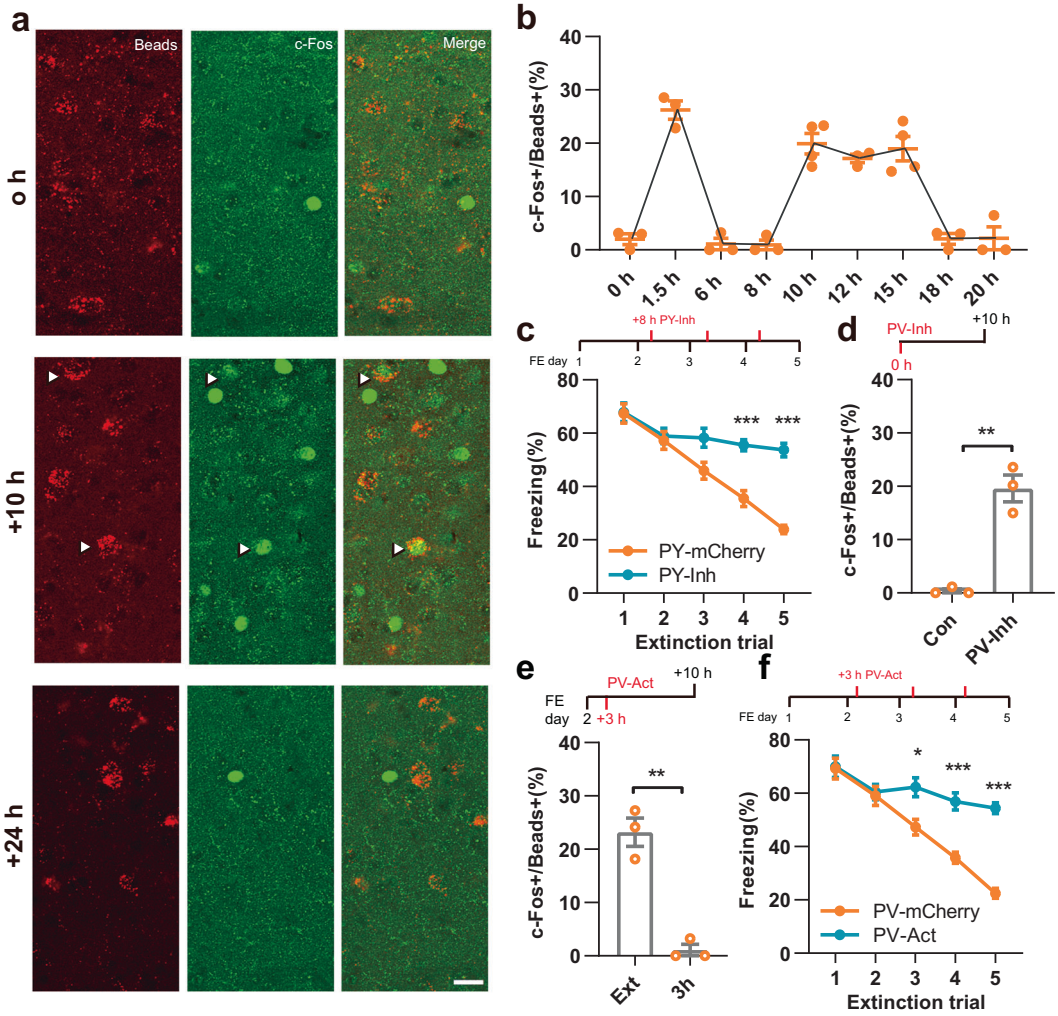

Fig. 6 BMA-projecting IL neuron activation depends on PV network configuration and contributes to fear extinction. a, **b** Time course of BMA-projecting IL neuron c-Fos expression following fear extinction trial 2. Arrowheads indicate the c-Fos+/beads+ cells; scale bar = 25 μm. **c** Chemogenetic inhibition of BMA-projecting IL neurons at +8 h impaired fear extinction. PY-Inh, AAV-DIO-hM4DGi-eYFP; PY-eYFP, AAV-DIO-eYFP ($n = 8$ mice for each group). Two-way repeated-measures ANOVA with Bonferroni's multiple comparisons test, group × time, $F(4,56) = 8.30$, $p < 0.0001$. **d** Chemogenetic inhibition of PV neurons increased BMA-projecting IL neuron c-Fos expression. $n = 3$ mice for each group, unpaired *t*-test (two-tailed), $t = 7.60$, df = 4, $P = 0.0016$. **e**, **f** Chemogenetic activation of PV neurons suppressed the second peak of c-Fos induction (**e**) and impaired fear extinction (**f**). **e** $n = 3$ mice for each group, unpaired *t*-test (two-tailed), $t = 7.69$, df = 4, $P = 0.0015$. **f** $n = 8$ and 9 mice for PV-eYFP and PV-Act, respectively; two-way repeated-measures ANOVA with Bonferroni's multiple comparisons test, group × time, $F(4,60) = 8.97$, $p < 0.0001$. Data are shown as the means ± SEM. $^*P < 0.05$, $^{**}P < 0.01$, $^{***}P < 0.001$. See Supplementary Table 1 for statistical details.

intracellular signalling cascades controlling the dedifferentiation of PV neurons might be triggered by endogenous NRG1-ErbB4 signalling before the appearance of the PV-state shift. However, the downstream cascades of NRG1-ErbB4 for the modulation of PV neuron differentiation are currently unknown and need to be further investigated in the future. We found that fear memory was gradually extinguished by extinction training at intervals of 24 and 48 h but not 72 h (Fig. 1a), which is consistent with the time course of extinction-induced NRG1 expression (Fig. 4b). Importantly, application of exogenous NRG1 at +3 h further facilitated fear extinction in mice subjected to 48 h interval training (Fig. 5c) and application at +48 h restored fear extinction in mice subjected to 72 h interval training (Fig. 5d). Thus, NRG1-ErbB4 signalling may represent a promising drug target for treating fear disorders.

The expression and processing of NRG1 are regulated by neuronal activity [48–50]. Enhanced neuronal activity in the IL induced by fear extinction (the first c-Fos peak) might stimulate NRG1 expression. NRG1 is widely expressed in pyramidal neurons, interneurons, astrocytes and microglia [51–53]. Meanwhile, NRG1 is available in various regions, including the hippocampus and amygdala [54–56], which are input regions of the mPFC [57, 58]. Of note, hippocampal or amygdala inputs to the mPFC are critical for fear-related behaviours [59–61]. Future studies need to explore whether PV network plasticity depends on endogenous NRG1 within the IL cortex or its inputs at the cellular level. A further finding in the present study is that NRG1 signalling in hippocampal CA1 promotes the training-induced low-PV state and facilitates memory retention in the IA task, whereas an ErbB4 antagonist induced the opposite effects, suggesting that NRG1 signalling-mediated PV plasticity is required for at least two different kinds of learning, fear extinction and IA.

Previous work has shown that neutralizing endogenous NRG1 and inhibiting or genetic ablation of ErbB4 reduce GABAergic transmission [62]. NRG1, by stimulating ErbB4, increases $GABA_A$ receptor-mediated synaptic currents [37] and enhances depolarization-induced GABA release [54]. These observations

suggest a role for NRG1-ErbB4 signalling in acute enhancement of GABAergic activity. Interestingly, we found that NRG1 induced a sustained low-PV configuration, whereas neutralizing endogenous NRG1, knocking down NRG1 or knocking out ErbB4 in PV neurons produced the opposite shift. Low-PV neurons represent the immature state of PV neurons and exhibit weakened functional outputs. Thus, our study provides the first demonstration that the long-lasting action (at least 48 h) of the NRG1-ErbB4 pathway may serve as a sustained modulation of local GABAergic activity, uncovering a novel role for NRG1-ErbB4 signalling in the adult brain.

Finally, we demonstrate that inhibition of BMA-projecting IL neurons impaired fear extinction. These data are consistent with reports suggesting that the mPFC exerts concerted top-down control over subcortical regions to tune the expression of fear [18, 26, 63]. Specifically, we found that the regulation of fear extinction by BMA-projecting IL neurons is dependent on PV network plasticity. Our data provide plausible circuit- and molecular-level explanations for the finding that activating BMA-projecting vmPFC neurons gave rise to stable extinction, whereas direct BMA activation only induced an acute effect on extinction [18]. Of note, there were some neurons expressing c-Fos in the IL upon learning that did not project to the BMA or CeA, and future studies should explore where they project and their roles. It also remains to be determined how defined populations of IL projection neurons are integrated into the local PV network and which cell types they contact in their long-range target structures, which would be an interesting topic for future studies.

In conclusion, we uncovered previously unknown molecular and local circuit mechanisms for mPFC-mediated top-down control of fear extinction. We found that sustained plasticity of the PV neuron network in the IL mPFC is required for fear extinction in adult mice, which is mediated by NRG1-ErbB4 signalling. Moreover, the regulation of fear extinction by BMA-projecting IL neurons is dependent on PV network configuration, suggesting alternative therapeutic approaches for treating fear disorders.

DATA AVAILABILITY

All data are available in the main text or the supplementary materials.

REFERENCES

1. Parsons RG, Ressler KJ. Implications of memory modulation for post-traumatic stress and fear disorders. Nat Neurosci. 2013;16:146–53.
2. Frankland PW, Bontempi B. The organization of recent and remote memories. Nat Rev Neurosci. 2005;6:119–30.
3. Squire LR, Bayley PJ. The neuroscience of remote memory. Curr Opin Neurobiol. 2007;17:185–96.
4. Neves G, Cooke SF, Bliss TV. Synaptic plasticity, memory and the hippocampus: a neural network approach to causality. Nat Rev Neurosci. 2008;9:65–75.
5. Martin SJ, Grimwood PD, Morris RG. Synaptic plasticity and memory: an evaluation of the hypothesis. Annu Rev Neurosci. 2000;23:649–711.
6. Rudy B, Fishell G, Lee S, Hjerling-Leffler J. Three groups of interneurons account for nearly 100% of neocortical GABAergic neurons. Dev Neurobiol. 2011;71:45–61.
7. Hu H, Gan J, Jonas P. Interneurons. Fast-spiking, parvalbumin(+) GABAergic interneurons: from cellular design to microcircuit function. Science. 2014;345:1255263.
8. Stark E, Eichler R, Roux L, Fujisawa S, Rotstein HG, Buzsaki G. Inhibition-induced theta resonance in cortical circuits. Neuron. 2013;80:1263–76.
9. Fagiolini M, Fritschy JM, Low K, Mohler H, Rudolph U, Hensch TK. Specific GABAA circuits for visual cortical plasticity. Science. 2004;303:1681–3.
10. Yazaki-Sugiyama Y, Kang S, Cateau H, Fukai T, Hensch TK. Bidirectional plasticity in fast-spiking GABA circuits by visual experience. Nature. 2009;462:218–21.
11. Levelt CN, Hubener M. Critical-period plasticity in the visual cortex. Annu Rev Neurosci. 2012;35:309–30.
12. Caroni P. Regulation of parvalbumin basket cell plasticity in rule learning. Biochem Biophys Res Commun. 2015;460:100–3.
13. Sotres-Bayon F, Cain CK, LeDoux JE. Brain mechanisms of fear extinction: historical perspectives on the contribution of prefrontal cortex. Biol Psychiatry. 2006;60:329–36.
14. Quirk GJ, Mueller D. Neural mechanisms of extinction learning and retrieval. Neuropsychopharmacology. 2008;33:56–72.
15. Morgan MA, Romanski LM, LeDoux JE. Extinction of emotional learning: contribution of medial prefrontal cortex. Neurosci Lett. 1993;163:109–13.
16. Milad MR, Quirk GJ. Neurons in medial prefrontal cortex signal memory for fear extinction. Nature. 2002;420:70–4.
17. Do-Monte FH, Manzano-Nieves G, Quinones-Laracuente K, Ramos-Medina L, Quirk GJ. Revisiting the role of infralimbic cortex in fear extinction with optogenetics. J Neurosci. 2015;35:3607–15.
18. Adhikari A, Lerner TN, Finkelstein J, Pak S, Jennings JH, Davidson TJ, et al. Basomedial amygdala mediates top-down control of anxiety and fear. Nature. 2015;527:179–85.
19. Peters J, Dieppa-Perea LM, Melendez LM, Quirk GJ. Induction of fear extinction with hippocampal-infralimbic BDNF. Science. 2010;328:1288–90.
20. Bukalo O, Pinard CR, Silverstein S, Brehm C, Hartley ND, Whittle N, et al. Prefrontal inputs to the amygdala instruct fear extinction memory formation. Sci Adv. 2015;1:e1500251.
21. Cho JH, Deisseroth K, Bolshakov VY. Synaptic encoding of fear extinction in mPFC-amygdala circuits. Neuron. 2013;80:1491–507.
22. Sananbenesi F, Fischer A, Wang X, Schrick C, Neve R, Radulovic J, et al. A hippocampal Cdk5 pathway regulates extinction of contextual fear. Nat Neurosci. 2007;10:1012–9.
23. Myers KM, Davis M. Mechanisms of fear extinction. Mol Psychiatry. 2007;12:120–50.
24. Karunakaran S, Chowdhury A, Donato F, Quairiaux C, Michel CM, Caroni P. PV plasticity sustained through D1/5 dopamine signaling required for long-term memory consolidation. Nat Neurosci. 2016;19:454–64.
25. Chattopadhyaya B, Di Cristo G, Wu CZ, Knott G, Kuhlman S, Fu Y, et al. GAD67-mediated GABA synthesis and signaling regulate inhibitory synaptic innervation in the visual cortex. Neuron. 2007;54:889–903.
26. DeNardo LA, Liu CD, Allen WE, Adams EL, Friedmann D, Fu L, et al. Temporal evolution of cortical ensembles promoting remote memory retrieval. Nat Neurosci. 2019;22:460–9.
27. Tasic B, Menon V, Nguyen TN, Kim TK, Jarsky T, Yao Z, et al. Adult mouse cortical cell taxonomy revealed by single cell transcriptomics. Nat Neurosci. 2016;19:335–46.
28. Armbruster BN, Li X, Pausch MH, Herlitze S, Roth BL. Evolving the lock to fit the key to create a family of G protein-coupled receptors potently activated by an inert ligand. Proc Natl Acad Sci USA. 2007;104:5163–8.
29. Conklin BR, Hsiao EC, Claeysen S, Dumuis A, Srinivasan S, Forsayeth JR, et al. Engineering GPCR signaling pathways with RASSLs. Nat Methods. 2008;5:673–8.
30. Pei Y, Rogan SC, Yan F, Roth BL. Engineered GPCRs as tools to modulate signal transduction. Physiology. 2008;23:313–21.
31. Donato F, Chowdhury A, Lahr M, Caroni P. Early- and late-born parvalbumin basket cell subpopulations exhibiting distinct regulation and roles in learning. Neuron. 2015;85:770–86.
32. Mei L, Xiong WC. Neuregulin 1 in neural development, synaptic plasticity and schizophrenia. Nat Rev Neurosci. 2008;9:437–52.
33. Chen YH, Lan YJ, Zhang SR, Li WP, Luo ZY, Lin S, et al. ErbB4 signaling in the prelimbic cortex regulates fear expression. Transl Psychiatry. 2017;7:e1168.
34. Wen L, Lu YS, Zhu XH, Li XM, Woo RS, Chen YJ, et al. Neuregulin 1 regulates pyramidal neuron activity via ErbB4 in parvalbumin-positive interneurons. Proc Natl Acad Sci USA. 2010;107:1211–6.
35. Fazzari P, Paternain AV, Valiente M, Pla R, Lujan R, Lloyd K, et al. Control of cortical GABA circuitry development by Nrg1 and ErbB4 signalling. Nature. 2010;464:1376–80.
36. Neddens J, Buonanno A. Selective populations of hippocampal interneurons express ErbB4 and their number and distribution is altered in ErbB4 knockout mice. Hippocampus. 2010;20:724–44.
37. Chen YJ, Zhang M, Yin DM, Wen L, Ting A, Wang P, et al. ErbB4 in parvalbumin-positive interneurons is critical for neuregulin 1 regulation of long-term potentiation. Proc Natl Acad Sci USA. 2010;107:21818–23.
38. Chen Y-H, Wu J-L, Hu N-Y, Zhuang J-P, Li W-P, Zhang S-R, et al. Distinct projections from the infralimbic cortex exert opposing effects in modulating anxiety and fear. J Clin Invest. 2021;131:e145692.
39. Kandel ER, Dudai Y, Mayford MR. The molecular and systems biology of memory. Cell. 2014;157:163–86.
40. Huang ZJ, Paul A. The diversity of GABAergic neurons and neural communication elements. Nat Rev Neurosci. 2019;20:563–72.
41. Trimble WS, Cowan DM, Scheller RH. VAMP-1: a synaptic vesicle-associated integral membrane protein. Proc Natl Acad Sci USA. 1988;85:4538–42.

42. Wada Y, Kitamoto K, Kanbe T, Tanaka K, Anraku Y. The SLP1 gene of Saccharomyces cerevisiae is essential for vacuolar morphogenesis and function. Mol Cell Biol. 1990;10:2214–23.
43. Robinson JS, Klionsky DJ, Banta LM, Emr SD. Protein sorting in Saccharomyces cerevisiae: isolation of mutants defective in the delivery and processing of multiple vacuolar hydrolases. Mol Cell Biol. 1988;8:4936–48.
44. Halachmi N, Lev Z. The Sec1 family: a novel family of proteins involved in synaptic transmission and general secretion. J Neurochem. 1996;66:889–97.
45. Maya Vetencourt JF, Sale A, Viegi A, Baroncelli L, De Pasquale R, O'Leary OF, et al. The antidepressant fluoxetine restores plasticity in the adult visual cortex. Science. 2008;320:385–8.
46. Dehorter N, Ciceri G, Bartolini G, Lim L, del Pino I, Marin O. Tuning of fast-spiking interneuron properties by an activity-dependent transcriptional switch. Science. 2015;349:1216–20.
47. Donato F, Rompani SB, Caroni P. Parvalbumin-expressing basket-cell network plasticity induced by experience regulates adult learning. Nature. 2013;504:272–6.
48. Eilam R, Pinkas-Kramarski R, Ratzkin BJ, Segal M, Yarden Y. Activity-dependent regulation of Neu differentiation factor/neuregulin expression in rat brain. Proc Natl Acad Sci USA. 1998;95:1888–93.
49. Ozaki M, Itoh K, Miyakawa Y, Kishida H, Hashikawa T. Protein processing and releases of neuregulin-1 are regulated in an activity-dependent manner. J Neurochem. 2004;91:176–88.
50. Tan GH, Liu YY, Hu XL, Yin DM, Mei L, Xiong ZQ. Neuregulin 1 represses limbic epileptogenesis through ErbB4 in parvalbumin-expressing interneurons. Nat Neurosci. 2011;15:258–66.
51. Liu X, Bates R, Yin DM, Shen C, Wang F, Su N, et al. Specific regulation of NRG1 isoform expression by neuronal activity. J Neurosci. 2011;31:8491–501.
52. Ikawa D, Makinodan M, Iwata K, Ohgidani M, Kato TA, Yamashita Y, et al. Microglia-derived neuregulin expression in psychiatric disorders. Brain Behav Immun. 2017;61:375–85.
53. Pankonin MS, Sohi J, Kamholz J, Loeb JA. Differential distribution of neuregulin in human brain and spinal fluid. Brain Res. 2009;1258:1–11.
54. Woo RS, Li XM, Tao Y, Carpenter-Hyland E, Huang YZ, Weber J, et al. Neuregulin-1 enhances depolarization-induced GABA release. Neuron. 2007;54:599–610.
55. Chen MS, Bermingham-McDonogh O, Danehy FT Jr, Nolan C, Scherer SS, Lucas J, et al. Expression of multiple neuregulin transcripts in postnatal rat brains. J Comp Neurol. 1994;349:389–400.
56. Law AJ, Shannon Weickert C, Hyde TM, Kleinman JE, Harrison PJ. Neuregulin-1 (NRG-1) mRNA and protein in the adult human brain. Neuroscience. 2004;127:125–36.
57. Ahrlund-Richter S, Xuan Y, van Lunteren JA, Kim H, Ortiz C, Pollak Dorocic I, et al. A whole-brain atlas of monosynaptic input targeting four different cell types in the medial prefrontal cortex of the mouse. Nat Neurosci. 2019;22:657–68.
58. Sun Q, Li X, Ren M, Zhao M, Zhong Q, Ren Y, et al. A whole-brain map of long-range inputs to GABAergic interneurons in the mouse medial prefrontal cortex. Nat Neurosci. 2019;22:1357–70.
59. Burgos-Robles A, Kimchi EY, Izadmehr EM, Porzenheim MJ, Ramos-Guasp WA, Nieh EH, et al. Amygdala inputs to prefrontal cortex guide behavior amid conflicting cues of reward and punishment. Nat Neurosci. 2017;20:824–35.
60. Marek R, Jin J, Goode TD, Giustino TF, Wang Q, Acca GM, et al. Hippocampus-driven feed-forward inhibition of the prefrontal cortex mediates relapse of extinguished fear. Nat Neurosci. 2018;21:384–92.
61. Klavir O, Prigge M, Sarel A, Paz R, Yizhar O. Manipulating fear associations via optogenetic modulation of amygdala inputs to prefrontal cortex. Nat Neurosci. 2017;20:836–44.
62. Lu Y, Sun XD, Hou FQ, Bi LL, Yin DM, Liu F, et al. Maintenance of GABAergic activity by neuregulin 1-ErbB4 in amygdala for fear memory. Neuron. 2014;84:835–46.
63. Dejean C, Courtin J, Rozeske RR, Bonnet MC, Dousset V, Michelet T, et al. Neuronal circuits for fear expression and recovery: recent advances and potential therapeutic strategies. Biol Psychiatry. 2015;78:298–306.

ACKNOWLEDGEMENTS

We thank Shuji Li, Yingying Fang and Ting Guo (Southern Medical University) for technological support. This work was supported by grants from the National Natural Science Foundation of China (grant numbers 82090032 and 31830033 to T.-M.G. and grant numbers 31801007 and 81881240049 to Y-HC), the Program for Changjiang Scholars and Innovative Research Team in University (grant number IRT_16R37 to T-MG), the Key-Area Research and Development Program of Guangdong Province (grant number 2018B030334001 to T-MG), the Guangdong Basic and Applied Basic Research Foundation (grant number 2020A1515011310 to Y-HC), the Guangdong-Hong Kong-Macao Greater Bay Area Centre for Brain Science and Brain-Inspired Intelligence Fund (grant number 2019019 to Y-HC), the Science and Technology Program of Guangzhou (grant number 202007030013, to T-MG) and the China Postdoctoral Science Foundation Grant (grant number 2020m682786 to N-YH).

AUTHOR CONTRIBUTIONS

T-MG and Y-HC designed the study. Y-HC and N-YH performed all experiments, except electrophysiological recordings with the help of D-YW, J-LW, L-LB, M-LW, J-TL, S-RZ and Y-LS. Z-YL and LH performed all electrophysiological recordings and analysed the electrophysiological data. Y-HC analysed all other data and generated the figures. X-WL provided technical support. T-MG and Y-HC interpreted the results with critical input from J-MY and S-ZZ. T-MG and Y-HC wrote the manuscript.

COMPETING INTERESTS

The authors declare no competing interests.

ADDITIONAL INFORMATION

Supplementary information The online version contains supplementary material available at https://doi.org/10.1038/s41380-021-01355-z.

Correspondence and requests for materials should be addressed to Tian-Ming Gao.

Reprints and permission information is available at http://www.nature.com/reprints

Publisher's note Springer Nature remains neutral with regard to jurisdictional claims in published maps and institutional affiliations.